Time-Varying Lower Bound of Interest Rates in Europe*

Jing Cynthia Wu
Chicago Booth and NBER

Fan Dora Xia
Bank for International Settlements

First draft: January 17, 2017
This draft: April 3, 2017

Abstract

We study the effectiveness of negative interest rate policy on the yield curve with a new shadow-rate term structure model. We price bonds with forward-looking agents in a model with a discrete policy rate and a non-constant spread between it and short term government bond yields. Our model matches the yield data, and we find increasing and decreasing the lower bound have asymmetric effects on the yield curve. A 10 basis-point drop in the lower bound lowers the 10-year yield by 6.5 to 8.5 basis points, and a 10 basis-point initial rise increases it by 9 to 14 basis points.

Keywords: effective lower bound, negative interest rates, shadow-rate term structure model, regime-switching model

*We thank Drew Creal, Jim Hamilton, Eric Swanson, and seminar and conference participants at Texas A&M University, University of Illinois Urbana-Champaign for helpful suggestions. Cynthia Wu gratefully acknowledges financial support from the James S. Kemper Foundation Faculty Scholar at the University of Chicago Booth School of Business. The views expressed herein are those of the authors and not necessarily the views of the BIS. Correspondence: cynthia.wu@chicagobooth.edu, dora.xia@bis.org.

1 Introduction

The effective lower bound (ELB) is one of the most discussed economic issues of the past decade. Central banks around the world repeatedly lowered their policy rates until they reached the zero lower bound (ZLB) in order to stimulate their economies as a response to negative shocks like the global financial crisis of 2007 - 2008. Zero was considered the lower bound for interest rates until recently when several central banks in Europe and the Bank of Japan adopted negative interest rate policies as a means of further encouraging investment and lending among financial institutions. For example, by the end of 2016, the deposit rate of the Swiss National Bank hit a record low of -0.75%, while the European Central Bank (ECB) lowered it to -0.4%.

What are the economic implications of negative interest rates? Do they provide the additional monetary easing that these economies need? Much of the existing literature has focused on whether and how much negative interest rate policy has affected banks' profitability; see, e.g. Borio et al. (2015), Jobst and Lin (2016), and Cœuré (2016). Our paper evaluates this policy's impact on the government bond yield curve, which links financial markets and the macroeconomy. The government bond market with negative interest rates is sizable and still growing. For example, by the end of 2016, the value of outstanding bonds with negative yields is over 10 trillion dollars. Understanding these questions is important to European countries and Japan, which are currently experiencing the ELB. It is also potentially important for the US economy, for which the ELB remains a future option if large negative shocks hit the economy.

We develop a new shadow-rate term structure model (SRTSM) to describe the current economic environment with negative interest rates. We apply our model to the Euro area, and investigate the effect of a change in the ELB on the yield curve. We find increasing and decreasing the lower bound have asymmetric effects on the yield curve. A 10-basis-point drop in the ELB lowers the short end of the yield curve by the same amount. The effect is dampened at longer maturities, and it decays to 6.5 to 8.5 basis points for the 10-year yield.

In contrast, a 10-basis-point rise in the ELB for the first time has the strongest effect on the medium maturities between 2 to 4 years, and it increases the 10-year yield by 9 to 14 basis points. The asymmetric responses have important policy implications: central banks might consider a slower pace when they plan to raise the ELB for the first time to avoid tightening financial conditions more than desirable.

The innovation of our model is the time-varying lower bound for interest rates, which consists of three main ingredients. First, agents are fully forward looking and incorporate their expectations about future movements in the lower bound when they price bonds. We are the first to introduce the forward-looking aspect of the time-varying lower bound into a model. This is crucial both theoretically and empirically. Forward-looking decision-making is arguably the most important building block of modern finance. A model with a time-varying lower bound would be internally inconsistent if agents in the model were naive, never updated their beliefs, and always thought the lower bound would stay where it currently was even after seeing it move repeatedly. Empirically, we find models with forward-looking agents fit the data better. More importantly, a model with myopic agents has different policy implications. In contrast to our main model with fully forward-looking agents, it implies a symmetric response of the yield curve to an increase or decrease in the lower bound. And, it suggests larger (smaller) effects of decreasing (increasing) the lower bound on long term yields than our main model.

Second, to capture the discrete nature of the deposit rate, we build a regime-switching process that allows us to preserve an analytical approximation for the pricing formula despite the additional flexibility introduced to accommodate the time-varying lower bound. Analytical bond prices make the model tractable and alleviate some numerical burdens. Dynamic term structure models are often criticized for their numerical behavior. If we had to compute bond prices numerically, the model would behave worse.

Third, we document a non-constant spread between the overnight policy rate and the short end of the government bond yield curve, and incorporate it into our model. This

empirical fact has been overlooked in the term structure literature. The short rate was higher than the deposit rate from mid 2013 to early 2015, and the difference was as large as 20 basis points. Since early 2015, the short rate - deposit rate spread has become negative and has grown over time. By the end of 2016, the difference became -60 basis points. A potential explanation for this negative spread toward the end of our sample is that government bonds issued by countries such as Germany and France are often posted as collateral for short-term borrowing in repo markets, and excessive cash in these economies leads to scarcity of these assets. Ignoring this inherent feature of the data could lead to a very poor fit.

We compare our model to several alternatives including popular specifications found in the literature. We find our proposed model performs the best in terms of higher likelihood, lower AIC and BIC, and lower pricing errors. All of the newly proposed modeling components are crucial to fit the forward curve or yield curve. The existing models in the literature, on the other hand, do poorly.

The implied shadow rate tracked the policy rate and the short end of the yield curve before the ELB was binding. It fluctuated between 0 and -1% when the policy lower bound was kept constant at zero. Subsequently, the ECB lowered the deposit rate at 10 basis-point intervals to -40 basis points. During this period, the shadow rate trended down, dropping from -1% to as low as -5%. The term premium for the Euro area has also trended down since 2009. A negative term premium emerged at the ELB, potentially due to QE purchases.

After a brief literature review, the rest of the paper proceeds as follows. Section 2 presents some simple empirical evidence on the relationship between the lower bound and yield curve. Section 3 sets up the new SRTSM. Section 4 lays out the details for the time-varying lower bound. Section 5 describes the estimation, Section 6 discusses empirical results, and Section 7 concludes.

Literature Earlier work has applied the SRTSM mostly to the Japanese and US yield curve. For example, Kim and Singleton (2012) and Ichiue and Ueno (2013) focus on Japan,

whereas Krippner (2013), Christensen and Rudebusch (2014), Wu and Xia (2016), and Bauer and Rudebusch (2016) focus on the United States. These papers kept the lower bound at a constant level.

A few studies have worked on the new development in Europe, where the policy lower bound kept moving down to negative numbers after it entered the ELB. For example, the online implementation of Wu and Xia (2016) for the Euro zone, and Lemke and Vladu (2016) and Kortela (2016). However, none of these papers allow agents to be forward-looking in terms of the lower bound. Moreover, the literature completely overlooks the non-constant spread between the policy rate and the government bond yield curve. We show both of these components are crucial to fit the yield curve as well as generate sensible economic implications.

Our paper relates to the regime-switching literature, with the seminal paper by Hamilton (1989). Applications of this class of model in the term structure literature include Ang and Bekaert (2002), Bansal and Zhou (2002), and Dai et al. (2007). The difference is that we focus on the regime shifts in the lower bound for interest rates, which is a newly developed phenomenon.

2 Empirical evidence

Since July 2012, the ECB has lowered the deposit rate to zero, entering the zero lower bound era (see the blue line in Figure 1). They subsequently moved the policy rate to be negative, replacing the ZLB with the ELB. The official level of the ELB prescribed by the central bank can be measured by the deposit rate. This section documents a positive and significant response of government bond yields to a change in the lower bound, using the 10-year yield for demonstration.

Figure 2 describes the relationship between the 10-year yield and the deposit rate. Blue dots are observations, and the red line is obtained by regressing the 10-year yield on the

Figure 1: Lower bound

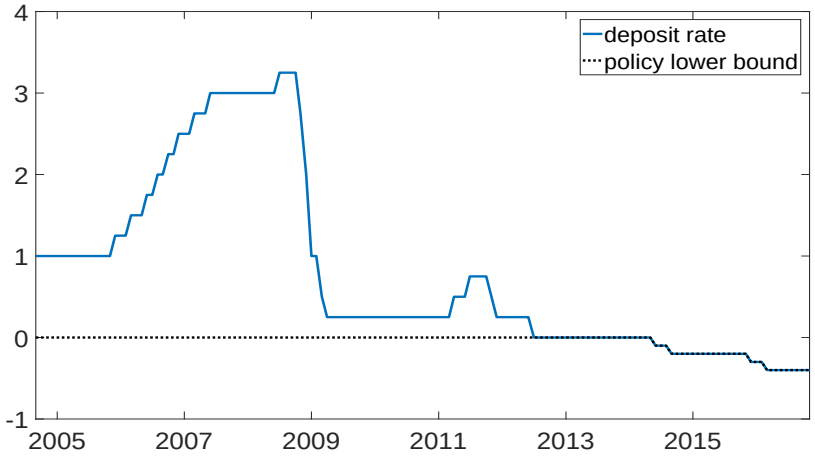

Notes: Blue dots: observations, red line: regression line. X-axis; deposit rates in percentage points; Y-axis: 10-year yield in percentage points. Sample spans from July 2012 to December 2016.

deposit rate. A higher lower bound is associated with higher long term interest rates. For example, when the lower bound is 0, the 10-year yield is about 2%, whereas a lower bound at -40 basis points is associated with 10-year yields around 0.

This relationship can also be captured by the following regression:

$$y_{120,t} = \beta_0 + \beta_1 r_t^d + \beta_2 X_t^{Macro} + e_t, \tag{2.1}$$

where $y_{120,t}$ is the yield of the zero-coupon bond with a maturity of 10 years, and r_t^d is the deposit rate. X_t^{Macro} controls for relevant macroeconomic variables, including inflation, the ECB's balance sheet as a percentage of GDP, industrial production (IP) growth, and unemployment rate. Table 1 shows that the coefficients on the deposit rate are positive across all model specifications, and all of them are statistically significant. This result is robust using other maturities, and it indicates that the movements in yields and the deposit rate are positively correlated even after controlling for these macro variables.

The qualitative relationship between the deposit rate and a yield with a specific maturity from the linear regression is robust. However, we are interested in the response of the

Figure 2: 10-year yield and deposit rate

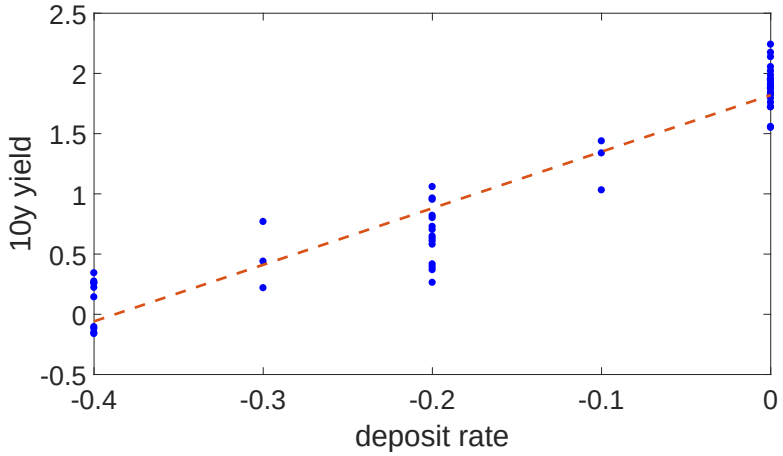

Notes: Top panel: time-series dynamics of the one-month yield in blue solid line and deposit rate in red dashed line; middle panel: the difference between the one-month yield and deposit rate. X-axis for these two panels: time. Sample spans from July 2012 to December 2016. Bottom panel: forward curve in December 2016 in blue solid line and deposit rate in dashed red line. X-axis for this panel: maturity in months.

whole yield curve, which should be priced internally consistently and without arbitrage opportunities. This and several other reasons explained below call for a new dynamic term structure model for a more formal quantitative analysis. First, the relationship between yields and macro variables becomes non-linear at the ELB. This is one of a few consensus reached in the literature about the ELB. Second, other factors that are important to the yield curve are not controlled for, which biases the results. Third, the regression model implies symmetric results whether the central bank raises or drops the deposit rate. To address these concerns, we build a new shadow rate term structure model in Sections 3 and 4.

3 A new shadow-rate term structure model

The time-varying lower bound in Figure 1 introduces new challenges for modeling the term structure of interest rates. Most existing models assume a constant lower bound. A few papers have introduced an exogenously moving lower bound. In these models, agents are myopic, and do not consider possible future changes of the lower bound. How to incorporate

Table 1: Regressing 10-year yield on the deposit rate and macro variables

Regressors	R1	R2	R3	R4
deposite rate	4.70	3.44	3.34	2.73
	(0.23)	(0.58)	(0.58)	(0.86)
inflation		0.30	0.38	0.34
		(0.11)	(0.13)	(0.13)
balance sheet (% of GDP)		-0.56	-0.65	-0.25
		(0.46)	(0.46)	(0.63)
IP growth			0.03	0.05
			(0.03)	(0.03)
Unemployment rate				0.20
				(0.21)

Notes: Regression coefficients and standard errors.

the forward-looking aspect into the model yet retain its tractability? This section and Section 4 propose a new term structure model that achieves these goals.

3.1 Setup

Following Black (1995), the short-term interest rate r_t is the maximum function of the shadow rate s_t and a lower bound. The innovation of our paper is that the lower bound for the government bond yield curve $\underline{r}_t$ is time varying, and relates to the short rate as follows:

$$r_t = \max\left(s_t, \underline{r}_t\right). \tag{3.1}$$

The shadow rate is an affine function of the latent yield factors, often labeled as "level," "slope," and "curvature":

$$s_t = \delta_0 + \delta_1' X_t,$$

whose physical dynamics follow a first-order vector autoregression (VAR):

$$X_t = \mu + \rho X_{t-1} + \Sigma\varepsilon_t,\ \ \varepsilon_t \sim N(0, I). \tag{3.2}$$

Similarly, the risk-neutral $\mathbb{Q}$ dynamics are

$$X_t = \mu^{\mathbb{Q}} + \rho^{\mathbb{Q}} X_{t-1} + \Sigma \varepsilon_t^{\mathbb{Q}},\ \varepsilon_t^{\mathbb{Q}} \sim N(0, I).$$

3.2 Bond prices

The no-arbitrage condition specifies that prices for zero-coupon bonds with different maturities are related by

$$P_{nt} = \mathbb{E}_t^{\mathbb{Q}} \left[\exp(-r_t) P_{n-1,t+1} \right].$$

The n-period yield relates to the price of the same asset as follows:

$$y_{nt} = -\frac{1}{n} \log(P_{nt}).$$

Following Wu and Xia (2016), we model forward rates rather than yields for the simplicity of the pricing formula. Define the one-period forward rate f_{nt} with maturity n as the return of carrying a government bond from $t+n$ to $t+n+1$ quoted at time t, which is a simple linear function of yields:

$$f_{nt} = (n+1) y_{n+1,t} - n y_{nt}.$$

Therefore, modeling forward rates is equivalent to modeling yields. Note that $f_{0t} = y_{1t} = r_t$.

3.2.1 Forward rates with a constant lower bound

If the lower bound were a constant $\underline{r}$, Wu and Xia (2016) show the forward rate can be approximated by

$$f_{nt} \approx \underline{r} + \tilde{\sigma}_n^{\mathbb{Q}} g \left(\frac{a_n + b_n' X_t - \underline{r}}{\tilde{\sigma}_n^{\mathbb{Q}}} \right), \tag{3.3}$$

where the function

$$g(z) = z\Phi(z) + \phi(z). \tag{3.4}$$

Inside the g function, $a_n + b_n' X_t$ is the n-period forward rate from the Gaussian affine term structure model. The coefficients a_n and b_n follow a set of difference equations whose solutions are

$$\begin{aligned} a_n &= \delta_0 + \delta_1' \left(\sum_{j=0}^{n-1} \left(\rho^{\mathbb{Q}}\right)^j \right) \mu^{\mathbb{Q}} - \frac{1}{2} \delta_1' \left(\sum_{j=0}^{n-1} \left(\rho^{\mathbb{Q}}\right)^j \right) \Sigma\Sigma' \left(\sum_{j=0}^{n-1} \left(\rho^{\mathbb{Q}}\right)^j \right)' \delta_1 \\ b_n' &= \delta_1' \left(\rho^{\mathbb{Q}}\right)^n. \end{aligned}$$

In addition, $(\tilde{\sigma}_n^{\mathbb{Q}})^2 \equiv \mathbb{V}_t^{\mathbb{Q}}(s_{t+n})$ is the conditional variance of the future shadow rate, and

$$(\tilde{\sigma}_n^{\mathbb{Q}})^2 = \sum_{j=0}^{n-1} \delta_1' (\rho^{\mathbb{Q}})^j \Sigma\Sigma' (\rho^{\mathbb{Q}\prime})^j \delta_1.$$

3.2.2 Forward rates with a time-varying lower bound

We are interested in the case where the lower bound is time-varying $\underline{r}_t$. Define the risk-neutral probability distribution for the lower bound n-periods later as $P_t^{\mathbb{Q}}(\underline{r}_{t+n})$. We will specify its dynamics in Section 4, and keep it implicit for now. The new pricing formula is

$$f_{nt} \approx \int \left(\underline{r}_{t+n} + \tilde{\sigma}_n^{\mathbb{Q}} g\left(\frac{a_n + b_n' X_t - \underline{r}_{t+n}}{\tilde{\sigma}_n^{\mathbb{Q}}} \right) \right) P_t^{\mathbb{Q}}(\underline{r}_{t+n}) d\underline{r}_{t+n}, \tag{3.5}$$

given that the factors X_t do not depend on r_t. See Appendix B.1 for the derivation.

Forward rates in (3.5) differ from (3.3) due to the time-varying lower bound. The new pricing formula (3.5) prices in the uncertainty associated with the future dynamics of the lower bound. The forward rate is calculated as an average of forward rates with known $\underline{r}_{t+n}$, weighted by the risk-neutral probability distribution of $\underline{r}_{t+n}$. If $\underline{r}_{t+n}$ were a constant, (3.5) becomes (3.3).

Note, in general, the integral in (3.5) needs to be solved numerically, which would introduce additional numerical burden when researchers estimate the model. How to specify the risk-neutral probability distribution $P_t^{\mathbb{Q}}(\underline{r}_{t+n})$ to preserve an analytical solution is the key. Section 4 will focus on the dynamics of the lower bound to achieve this goal.

4 Time-varying lower bound

This section proposes a novel model for the time-varying lower bound. First, we model the component of the lower bound that is driven by monetary policy. Due to its discrete nature, we propose a regime-switching model. Then, we inspect the spread between the overnight policy rate and the government yield curve. Our agents are fully forward looking, incorporating potential changes of the future lower bound into bond prices. Although our model is more flexible in order to accommodate features in the data, it still allows an analytical approximation for bond prices. Having analytical bond prices is crucial for the tractability and better numerical behavior of the model. In Section 6, we will demonstrate our model's ability to fit the data.

4.1 Policy lower bound

Much of the government bond yield curve is driven by monetary policy. In this section, we investigate the policy-driven component of the time-varying lower bound. We inspect empirical features of the policy rate, and use them to inform a regime-switching model.

The deposit rate r_t^d in Figure 1 is a natural candidate for the policy lower bound $\underline{r}_t^d$ when the economy was binding at the ELB. We formalize the concept of the policy lower bound as follows:

$$\begin{cases} \underline{r}_t^d = 0, \text{ if not ELB} \\ \underline{r}_t^d = r_t^d, \text{ if ELB,} \end{cases} \tag{4.1}$$

and plot it in the black dotted line in Figure 1.

Simple facts The first empirical observation from Figure 1 is that the policy lower bound is discrete and takes multiples of -10 basis points. In the data, we have observed it takes the value of 0, -10, -20, -30, and -40 basis points. In the model, we assume its maximum value is 0 and its minimum is $-\underline{R}$:

$$\underline{r}_t^d \in \{0, -10, ..., -\underline{R}\} \text{ basis points.} \tag{4.2}$$

Another observation from Figure 1 is the policy lower bound moves 10 basis points at a time, if it moves. Moreover, for most of the time, it stays constant. In the data, we only see the lower bound decrease. In the future, we expect the lower bound to eventually move back up to zero. Hence,

$$\underline{r}_t^d | \underline{r}_{t-1}^d \in \{\underline{r}_{t-1}^d - 10, \underline{r}_{t-1}^d, \underline{r}_{t-1}^d + 10\}. \tag{4.3}$$

Momentum Equation (4.3) captures the persistence in the policy lower bound in the sense that the lower bound could stay where it was. Another type of persistence exists in terms of whether the policy lower bound or deposit rate is moving downward or upward. For example, when a broad downward trend occurs, as we have experienced since the onset of the ELB, it is more likely to keep moving down than up. This demonstrates the momentum of the lower-bound movements. We formalize this idea by introducing Δ_t, which describes the direction in which the lower bound is moving. $\Delta_t = \pm 1$, where $\Delta_t = +1$ is the up state and $\Delta_t = -1$ is the down state. The lower bound $\underline{r}_t^d$ might stay constant for a period of time between two downward movements, and we still refer to this period as the down state $\Delta_t = -1$. More specifically, we define it as follows:

Definition 1 *When* $r_t^d > -\underline{R}$, $\Delta_t = -1$ *if* $\exists n > 0$ *such that* $r_t^d < r_{t-n}^d$ *and* $r_t^d = r_{t-j}^d \forall 0 < j < n$; *otherwise,* $\Delta_t = +1$. *When* $r_t^d = -\underline{R}$, $\Delta_t = \pm 1$.

Table 2: Conditional transition probability $P^{\mathbb{Q}}(\underline{r}_t^d|\underline{r}_{t-1}^d, \Delta_t)$

	$\underline{r}_t^d$ \ $\underline{r}_{t-1}^d$	$-\underline{R} < \underline{r}_{t-1}^d < 0$	$-\underline{R}$	0
$\Delta_t = +1$	$\underline{r}_{t-1}^d - 10$	0	0	0
	$\underline{r}_{t-1}^d$	π	π	1
	$\underline{r}_{t-1}^d + 10$	$1-\pi$	$1-\pi$	0
$\Delta_t = -1$	$\underline{r}_{t-1}^d - 10$	$1-\pi$	0	0
	$\underline{r}_{t-1}^d$	π	1	1
	$\underline{r}_{t-1}^d + 10$	0	0	0

Figure 1 demonstrates the down state is persistent or has momentum. This can be extended to the up state as well. We capture this persistence with the following risk-neutral dynamics:

$$P^{\mathbb{Q}}(\Delta_t = \Delta_{t-1}|\Delta_{t-1}) = p, \tag{4.4}$$

where $p \approx 1$ describes a down state is most likely followed by another down state, which is consistent with the data. $P^{\mathbb{Q}}(\Delta_t \neq \Delta_{t-1}|\Delta_{t-1}) = 1 - p$ is the probability of changing the direction.

Conditional distribution of lower bound Equation (4.3) and Definition 1 imply that if we are in the $\Delta_t = -1$ state, the lower bound can only stay where it was $\underline{r}_t^d = \underline{r}_{t-1}^d$ or move down by 10 basis points $\underline{r}_t^d = \underline{r}_{t-1}^d - 10$. Similarly, if $\Delta_t = +1$, then $\underline{r}_t^d = \underline{r}_{t-1}^d$ or $\underline{r}_t^d = \underline{r}_{t-1}^d + 10$. We formalize this idea by specifying the conditional transition probability $P^{\mathbb{Q}}(\underline{r}_t^d|\underline{r}_{t-1}^d, \Delta_t)$ in Table 2. Per (4.3), the lower bound does not always move. We allow for a probability π that the lower bound stays the same, and $\pi \approx 1$. Next, per (4.2), the lower bound is not allowed to go above 0 or below $-\underline{R}$. Therefore, when $\Delta_t = -1$ and $\underline{r}_{t-1}^d = -\underline{R}$, all the probability mass concentrates at staying. We make $\underline{r}_t^d = 0$ an absorbing state, that is, $\underline{r}_t^d = 0$ if $\underline{r}_{t-1}^d = 0$, to capture the long history of the lower bound at zero.

Marginal distribution of lower bound From (3.5), the probability distribution of interest for pricing purposes is the risk-neutral probability distribution of the lower bound n periods into the future. It can be written as the sum of the joint distributions of the lower bound and directional states:

$$P_t^{\mathbb{Q}}(\underline{r}_{t+n}^d) = \sum_{\Delta_{t+n}} P_t^{\mathbb{Q}}(\underline{r}_{t+n}^d, \Delta_{t+n}), \tag{4.5}$$

and the right-hand side has the following dynamics:

$$\begin{aligned} & P_t^{\mathbb{Q}}(\underline{r}_{t+n}^d, \Delta_{t+n}) \\ = & \sum_{\underline{r}_{t+n-1}^d, \Delta_{t+n-1}} P_t^{\mathbb{Q}}(\underline{r}_{t+n}^d, \Delta_{t+n} | \underline{r}_{t+n-1}^d, \Delta_{t+n-1}) P_t^{\mathbb{Q}}(\underline{r}_{t+n-1}^d, \Delta_{t+n-1}), \end{aligned} \tag{4.6}$$

where the transition probability can be decomposed as follows:

$$\begin{aligned} & P_t^{\mathbb{Q}}(\underline{r}_{t+n}^d, \Delta_{t+n} | \underline{r}_{t+n-1}^d, \Delta_{t+n-1}) \\ = & P_t^{\mathbb{Q}}(\underline{r}_{t+n}^d | \underline{r}_{t+n-1}^d, \Delta_{t+n}, \Delta_{t+n-1}) P_t^{\mathbb{Q}}(\Delta_{t+n} | \underline{r}_{t+n-1}^d, \Delta_{t+n-1}) \\ = & P^{\mathbb{Q}}(\underline{r}_{t+n}^d | \underline{r}_{t+n-1}^d, \Delta_{t+n}) P^{\mathbb{Q}}(\Delta_{t+n} | \Delta_{t+n-1}), \end{aligned} \tag{4.7}$$

and the two components are defined in (4.4) and Table 2. The matrix form of the joint dynamics (4.6) is in Appendix A.

4.2 Spread

So far, we have laid out two lower bound concepts. We introduced the lower bound for the government bond $\underline{r}_t$ in Section 3. In Subsection 4.1, we built a model for its main component: the policy lower bound $\underline{r}_t^d$. In a world without frictions, these rates should be identical. In practice, they are not perfect substitutes due to some institutional details. For example, some financial institutions cannot access reserves, which creates a wedge between the two.

Figure 3: Spread

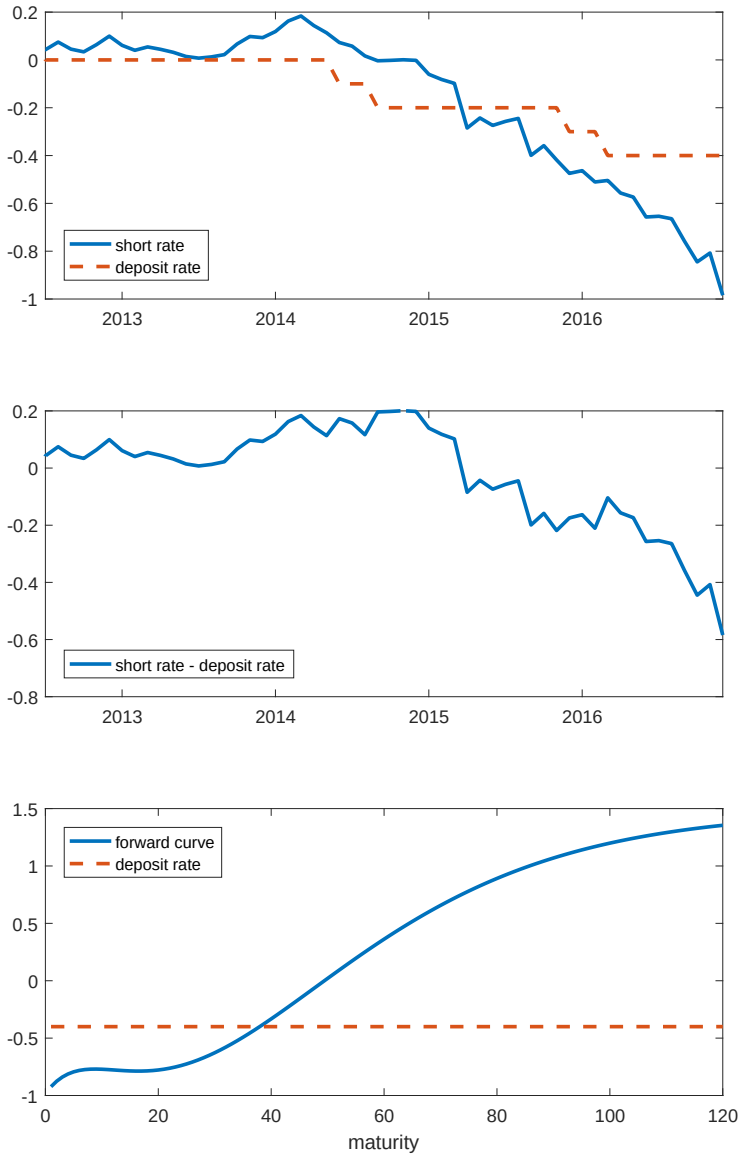

Notes: Top panel: time-series dynamics of the one-month yield in blue solid line and deposit rate in red dashed line; middle panel: the difference between the one-month yield and deposit rate. X-axis for these two panels: time. Sample spans from July 2012 to December 2016. Bottom panel: forward curve in December 2016 in blue solid line and deposit rate in dashed red line. X-axis for this panel: maturity in months.

Figure 3 plots the time-series dynamics of the one-month short-term interest rate and deposit rate in the top panel, and their difference in the middle. At the beginning of the ELB period, the two rates were very similar to each other, as theory suggests. However, the difference grew over time. The spread was positive from mid 2013 to early 2015, and at the peak, the short rate was 20 basis points higher than the deposit rate.

Since early 2015, the short rate - deposit rate spread has become negative and has grown over time. By the end of 2016, the difference became -60 basis points. One explanation for this negative spread toward the end of our sample is that government bonds issued by countries such as Germany and France are often posted as collateral for short-term borrowing in repo markets, and excessive cash in these economies leads to scarcity of these assets.

The bottom panel of Figure 3 plots the cross section of the forward curve in December 2016. The front end of the curve was at -90 basis points, whereas the deposit rate was only -40 basis points. Note the discrepancy between government bond interest rates and the deposit rate is not limited to the very short end. Rather, it extends to all the maturities.

To capture this fundamental feature of the data, we introduce a spread into our model, and model the lower bound for the government bond as the sum of the policy lower bound and a spread[1]:

$$\begin{cases} \underline{r}_t = 0, \text{ if not ELB} \\ \underline{r}_t = \underline{r}_t^d + sp_t, \text{ if ELB,} \end{cases} \tag{4.8}$$

where the spread sp_t follows an AR(1) with mean 0 under the risk-neutral measure:

$$sp_t \quad = \quad \rho_{sp} sp_{t-1} + e_t, \;\; e_t \sim N(0, \sigma_{sp}^2). \tag{4.9}$$

[1]We estimated a constant lower bound using the sample from September 2004 to May 2014, and the estimate is essentially 0.

4.3 Bond prices

With the dynamics of the lower bound specified in Subsections 4.1 - 4.2, the pricing formula in (3.5) becomes

$$f_{nt} \approx \sum_{\underline{r}^d_{t+n}} P_t^{\mathbb{Q}}(\underline{r}^d_{t+n}) \left(\underline{r}^d_{t+n} + c_n sp_t + \sigma_n^{\mathbb{Q}} g \left(\frac{a_n + b_n' X_t - \underline{r}^d_{t+n} - c_n sp_t}{\sigma_n^{\mathbb{Q}}} \right) \right), \quad (4.10)$$

where $c_n = \rho_{sp}^n; (\sigma_n^{\mathbb{Q}})^2 = (\tilde{\sigma}_n^{\mathbb{Q}})^2 + (\sum_{j=0}^{n-1} \rho_{sp}^{2j})\sigma_{sp}^2$. See Appendix B.2 for the derivation.

The integral in (3.5) is replaced by the summation in (4.10). The regime-switching dynamics for the discrete policy lower bound and the AR process for the spread together preserve the analytical approximation for the pricing formula. Having an analytical approximation is crucial for the model to be tractable and have better numerical behavior. Dynamics term structure models are often criticized for being difficult to estimate. For example, in the class of Gaussian affine term structure model which is a special case of our model when $\underline{r}_t \to \infty$ and has analytical bond prices, a literature has been dedicated to improving the model's performance: See Joslin et al. (2011), Christensen et al. (2011), Hamilton and Wu (2012b), Adrian et al. (2012), Creal and Wu (2015), and de Los Rios (2015). If we had to compute bond prices numerically, the model would behave worse.

5 Estimation

We construct 3- and 6-month-ahead and 1-, 2-, 5-, 7-, and 10-year-ahead 1-month forward rates for AAA-rated government bond yields in the Euro area; the dataset is available on the ECB's website.[2] Our sample is monthly from September 2004 to December 2016. We date the ELB period when the deposit rate is zero and below, and it starts from July 2012.

For the new part of the model detailed in Section 4, we pool information from the physical dynamics and risk-neutral dynamics together in our main specification due to the

[2]These forward rates map into f_{nt} in (3.5) with $n = 3, 6, 12, 24, 60, 84, 120$.

short sample. Specifically, the physical dynamics are the same as the risk-neutral dynamics specified in Section 4. This assumption will be relaxed in the extension in Subsection 6.4, and all of our main results hold.

The state variables $\underline{r}_t^d$, Δ_t are measured according to (4.1) and Definition 1. Conditioning on $\underline{r}_t^d$, Δ_t, we express our SRTSM with a time-varying lower bound as a nonlinear state-space model. The transition equations include (3.2) and (4.9), which describe the dynamics of the latent factors. (4.10) relates the model-implied forward rate f_{nt} to the state variables. Adding measurement errors, the measurement equation for the observed forward rate f_{nt}^o becomes

$$f_{nt}^o = \sum_{\underline{r}_{t+n}^d} P_t^{\mathbb{Q}}(\underline{r}_{t+n}^d) \left(\underline{r}_{t+n}^d + c_n sp_t + \sigma_n^{\mathbb{Q}} g\left(\frac{a_n + b_n' X_t - \underline{r}_{t+n}^d - c_n sp_t}{\sigma_n^{\mathbb{Q}}} \right) \right) + \eta_{nt}, \tag{5.1}$$

where the measurement error η_{nt} is i.i.d. normal, $\eta_{nt} \sim N(0, \omega^2)$.

The collection of parameters we estimate consists of three subsets: (1) parameters related to $\underline{r}_t$ and Δ_t, including (p, π); (2) parameters describing the dynamics of sp_t, including (ρ_{sp}, σ_{sp}); and (3) parameters related to X_t, including $(\mu, \mu^{\mathbb{Q}}, \rho, \rho^{\mathbb{Q}}, \Sigma, \delta_0, \delta_1)$. For identification, we impose restrictions on parameters in the last group similar to Hamilton and Wu (2014): (i) $\delta_1 = [1, 1, 1]'$, (ii)$\mu^{\mathbb{Q}} = 0$, (iii) $\rho^{\mathbb{Q}}$ is diagonal with eigenvalues in descending order, and (iv) Σ is lower triangular.

We use maximum likelihood estimation with the extended Kalman filter. See Appendix C for details. In our implementation, we set $-\underline{R} = -100$ basis points. We report maximum likelihood estimates and robust standard errors (see Hamilton (1994)) in Table 3. The eigenvalues of ρ, $\rho^{\mathbb{Q}}$ indicate the factors X_t are highly persistent under both measures. This finding is consistent with the term structure literature. The lower-bound dynamics are also persistent. Δ_t has a 96% chance of staying the same, for example, from a down state to another down state. The chance for the lower bound to stay where it was is 97%. The spread sp_t almost follows a random walk. Other parameters controlling level and scale are comparable to what we see in the literature.

Table 3: Maximum likelihood estimates

1200μ	-0.8332	0.5264	-0.1014	$1200\mu^{\mathbb{Q}}$	0	0	0
	(0.3157)	(0.3588)	(0.4875)				
ρ	0.9661	0.0121	-0.0080	$\rho^{\mathbb{Q}}$	0.9985	0	0
	(0.0117)	(0.0560)	(0.0695)		(0.0005)		
	0.0318	1.1199	0.2041		0	0.9666	0
	(0.0130)	(0.2419)	(0.2698)			(0.0032)	
	-0.0155	-0.1381	0.7818		0	0	0.9249
	(0.0190)	(0.2620)	(0.2935)				(0.0155)
$\lvert eig(\rho)\rvert$	0.9993	0.9345	0.9345				
δ_0	23.3840						
	(0.2115)						
p	0.9629						
	(0.0033)						
π	0.9697						
	(0.0064)						
ρ_{sp}	0.9996						
	(0.0004)						
1200Σ	0.7987	0	0				
	(0.1461)						
	-0.4183	1.4792	0				
	(0.2763)	(0.2551)					
	-0.1042	-1.5064	0.3401				
	(0.3358)	(0.2114)	(0.1070)				
$1200\sigma_{sp}$	0.0499						
	(0.0136)						
1200ω	0.0655						
	(0.0058)						

Notes: Maximum likelihood estimates with quasi-maximum likelihood standard errors in parentheses. Sample: September 2004 to December 2016.

Figure 4 plots the spread filtered from our model in blue, and compares it with two proxies constructed from the observed data. The first proxy in the red dotted line is the difference between the 3-month forward rate and the deposit rate, where three months is the shortest maturity used in our sample. They closely track each other, with a high correlation at 0.96. The second proxy takes the difference between the short rate and the deposit rate, as suggested by the model. Although the short rate is not in our information set when we estimate the model, the observed and filtered spreads are again very close to each other.

Figure 4: Spread

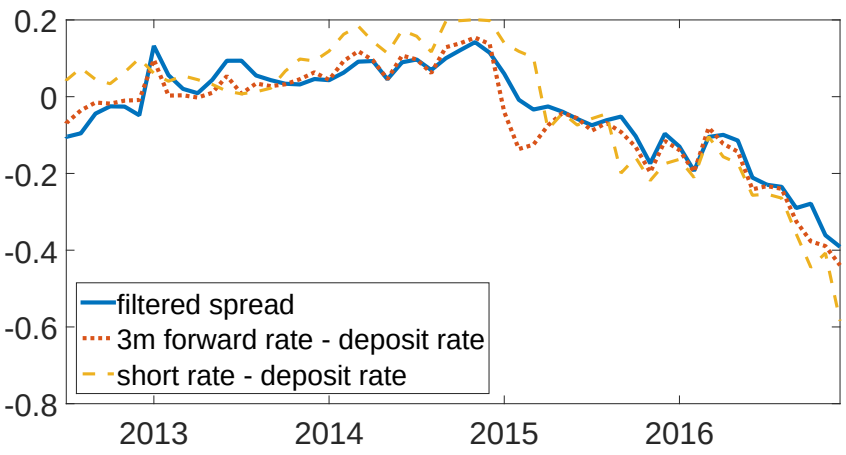

Notes: Blue solid line: filtered spread; red dotted line: the spread between the 3-month forward rate and the deposit rate; yellow dashed line: the spread between the short rate and the deposit rate. X-axis: time. Sample spans from July 2012 to December 2016.

6 Economic implications

Subsection 6.1 conducts counterfactual policy analyses to see the effect of changing the ELB on the yield curve. We then show the importance of correctly specifying the lower bound process in Subsection 6.2. We compare our main model as laid out in Sections 3 - 4 with alternative specifications for the lower bound. Subsections 6.3 - 6.4 discuss the implied shadow rate and term premia.

6.1 Counterfactual policy analyses

In this section, we conduct counterfactual policy analyses to study the impact of changing the ELB on the yield curve. First, we ask how the yield curve would react if we lowered the ELB by another 10 basis points. Second, as economic outlook improves, central banks would gradually unwind unconventional monetary policy. Increasing the ELB is one of the tools at their disposal. Hence, the arguably more interesting question is how the yield curve would react if the ECB decided to increase the ELB for the first time. We conduct these experiments by explicitly holding other factors affecting the yield curve constant.

Figure 5: Impact of lowering ELB on the yield curve

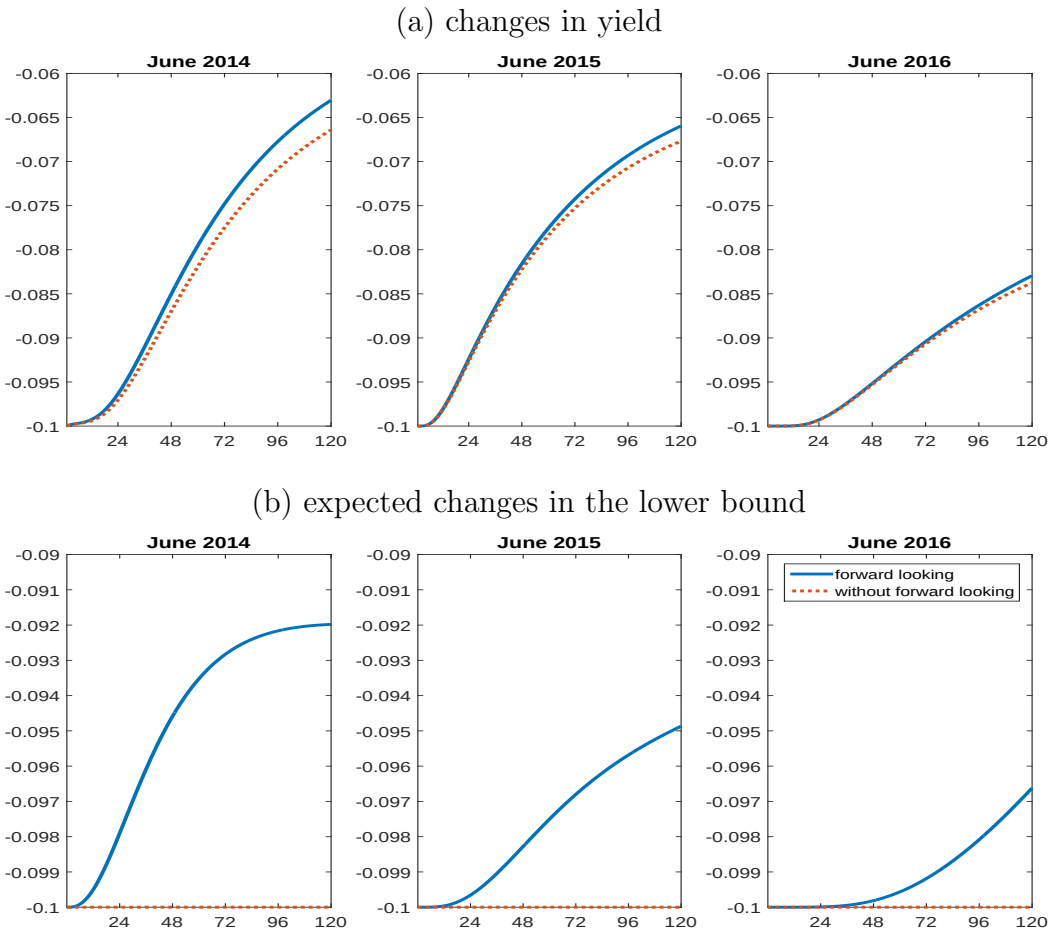

Notes: Panel (a): changes in the yield curve in response to lowering the ELB by 10 basis points. Panel (b): expected changes in the lower bound. Blue lines: agents are forward looking; red dashed lines: agents are not forward looking. X-axis: maturity in months; Y-axis: interest rates in percentage points.

The top panel of Figure 5 plots reactions of the yield curve to a lower ELB across three different dates, and the responses from our main model are in the blue lines. By lowering the ELB by 10 basis points, the short end of the curve subsequently decreases by 10 basis points as well. This effect is dampened when maturity increases. At the 10-year horizon, the change decays to about 6.5 to 8.5 basis points.

We plot in red dashed lines what happens when agents are myopic expecting the future lower bound to be equal to its current value. The effect on the longer end of the yield curve is less when agents are forward looking, because they expect the lower bound to revert to its

Figure 6: Impact of initial increase in the ELB on the yield curve

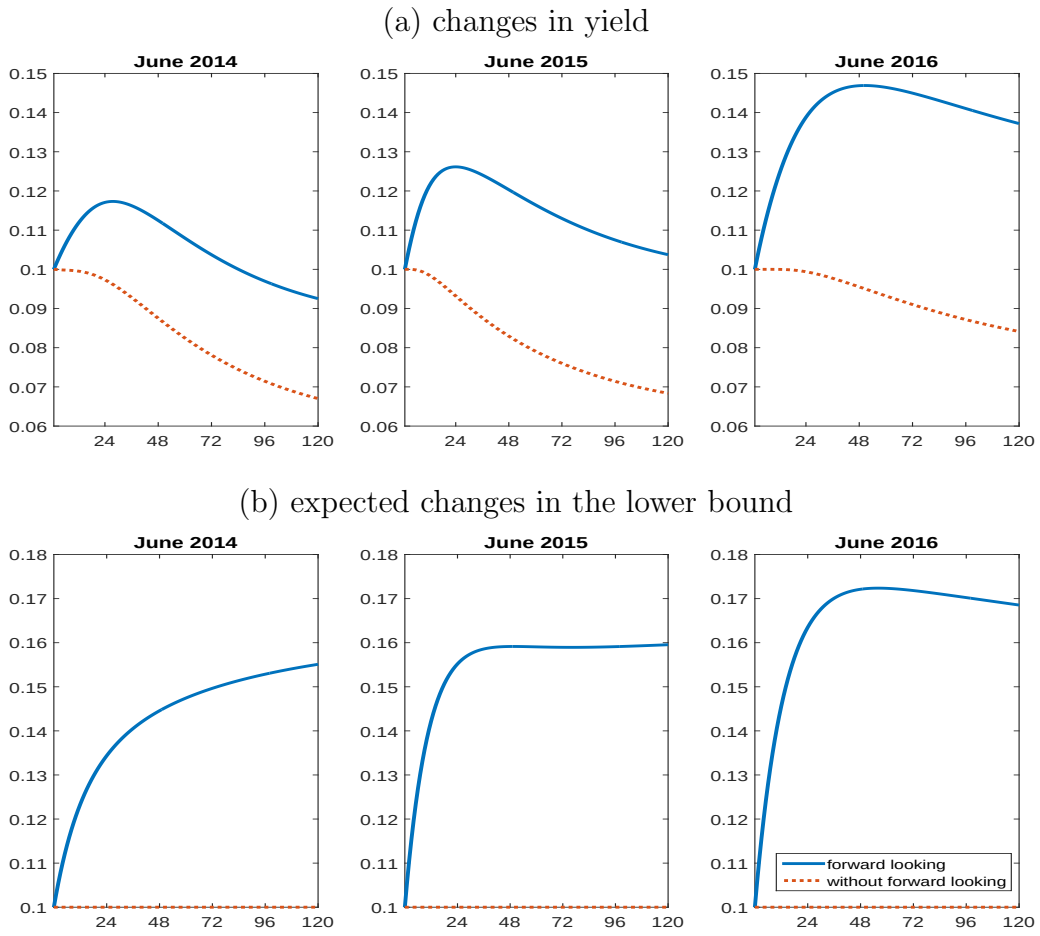

Notes: Panel (a): changes in the yield curve in response to increasing the ELB for the first time by 10 basis points. Panel (b): expected changes in the lower bound. Blue lines: agents are forward looking; red dashed lines: agents are not forward looking. X-axis: maturity in months; Y-axis: interest rates in percentage points.

unconditional mean in the long run, whereas naive agents think the 10-basis-point change in the lower bound is permanent. The expected changes in the lower bound are illustrated in the bottom panel.

Next, we conduct an experiment in Figure 6 of raising the ELB for the first time by 10 basis points, and results from our main model are in blue. Interestingly, increasing and decreasing the ELB have asymmetric implications for the yield curve. More specifically, the impact of increasing the ELB peaks at medium maturities between 2 to 4 years. It is also

larger: the 10 year yield increases by 9 to 14 basis points in response. These asymmetric responses have important policy implications. Central banks might consider a slower pace when they plan to raise the ELB for the first time to avoid tightening financial conditions more than desirable.

There are two economic forces contributing to the asymmetry. First, when the ELB increases for the first time, Δ_t changes from the down state to the up state by definition. The momentum factor leads expected changes of the lower bound in the bottom panel larger than 10 basis points. Second, similar to the channel explaining Figure 5, the lower bound's impact on the yield curve decreases as maturity increases. These two forces together contribute to this asymmetry and hump shape.

The model with (in blue) and without (in red) forward-looking agents differ significantly in this case, demonstrating the importance of the forward-looking aspect. Moreover, the model with myopic agents has symmetric implications whether the central bank lowers (in Figure 5) or raises (in Figure 6) the ELB.

6.2 Model comparison

Alternative specifications We show the importance of our new modeling ingredients by comparing our main model M_{main} with alternative model specifications described in Table 4. Models M_{BM-TV}, M_{BM-0}, and M_{BM-40} are the benchmarks in the literature. None of them allow (1) a regime-switching process for the policy lower bound, (2) a non-constant spread between the policy rate and the yield curve, or (3) forward-looking agents in terms of future changes in the lower bound.

M_{BM-TV} does allow an exogenously varying lower bound tracking the deposit rate, and is consistent with the online implementation of Wu and Xia (2016) for the Euro zone, and similar to Lemke and Vladu (2016) and Kortela (2016). M_{BM-0} and M_{BM-40}, on the other hand, have a constant lower bound, consistent with most SRTSM papers on the US yield curve. For example, see Christensen and Rudebusch (2014), Wu and Xia (2016), and Bauer

Table 4: Model specifications

	short description	full description
M_{main}	main model	The model is specified in Sections 3 - 4. The government bond lower bound $\underline{r}_t$ consists of the regime-switching policy lower bound $\underline{r}_t^d$ and a non-constant spread sp_t as in (4.8). Agents are fully forward looking.
M_{BM-TV}	benchmark with exogenously moving lower bound	The policy lower bound $\underline{r}_t^d$ is exogenously moving. But agents are not forward looking and think the future lower bound would stay where it is today. Also, $sp_t = 0$. This specification is similar to the models in the literature. See the online implementation of Wu and Xia (2016) for the Euro area, and Lemke and Vladu (2016), and Kortela (2016).
M_{BM-0}	benchmark with a constant lower bound at 0	This model has a constant lower bound at 0, completely removing any time variation in the lower bound, and is another benchmark model in the literature. For example, see Christensen and Rudebusch (2014), Wu and Xia (2016), and Bauer and Rudebusch (2016).
M_{BM-40}	benchmark with a constant lower bound at -40 b.p.	This model is the same as the previous one, except the lower bound is changed to -40 basis points.
M_{RS}	model with only regime switching	The policy lower bound $\underline{r}_t^d$ follows the regime-switching process, and agents are forward looking, but $sp_t = 0$.

and Rudebusch (2016). The difference between them are the level of the lower bound: it is naively chosen at 0 for M_{BM-0}, and -40 basis points for M_{BM-40} as the lowest point of the deposit rate.

To single out the contributions of the regime-switching policy lower bound and the spread, we also introduce an intermediate model M_{RS}. It is our main model excluding the spread: $sp_t = 0$. The comparison between this model and the benchmark models tells us how much improvement comes from the regime-switching policy lower bound alone. The difference between this model and our main model further shows the contribution of adding the spread. Details for these models can be found in Appendix C.3.

Performance of our main model Table 5 compares these models in terms of log likelihood values, information criteria, and measurement errors. Our main model M_{main} yields

Table 5: Model comparison

		M_{main}	M_{BM-TV}	M_{BM-0}	M_{BM-40}	M_{RS}
full sample	log likelihood	**693.46**	466.06	59.20	438.57	605.29
	AIC	**-1332.92**	-886.12	-72.40	-831.14	-1160.58
	BIC	**-1195.85**	-769.36	44.37	-714.37	-1033.66
	Measurement errors					
	3m	**3.85**	9.50	23.05	8.97	6.71
	6m	**3.67**	8.95	21.57	7.93	5.26
	1y	**5.14**	10.28	23.17	10.17	6.20
	2y	4.93	8.91	25.83	8.21	**4.92**
	5y	**6.68**	7.73	12.76	8.34	7.49
	7y	**3.36**	4.47	9.00	4.52	3.54
	10y	**8.07**	8.58	12.89	8.92	8.96
ELB	3m	**4.64**	14.30	36.59	12.88	9.95
	6m	**3.27**	13.48	34.51	11.76	6.63
	1y	**3.36**	13.74	35.71	12.37	5.65
	2y	**5.43**	13.07	38.92	11.82	5.52
	5y	**5.17**	7.31	16.97	8.34	7.36
	7y	**3.62**	4.57	11.62	4.31	4.07
	10y	**6.59**	8.50	14.74	9.02	8.78

Notes: Top panel: full sample from September 2004 to December 2016; bottom panel: ELB sample from July 2012 to December 2016. First column: our main model M_{main}; second column: benchmark model M_{BM-TV} with exogenously varying lower bound; third column: benchmark model M_{BM-0} with a constant lower bound at zero; fourth column: benchmark model M_{BM-40} with a constant lower bound at -40 basis points; fifth column: M_{RS} without spread; Conditional log likelihood, conditioning on the observed $\Delta_{1:T}, \underline{r}^d_{1:T}$, and corresponding AIC and BIC are reported for the full sample. Measurement errors are in basis points, and computed as the root-mean-square errors between observed and model-implied forward rates with maturities from 3 months to 10 years. We highlight the smallest measurement errors, AIC and BIC, and the highest log likelihood value.

the highest likelihood value. It also has the smallest AIC and BIC, where the information criteria penalize overparameterization. These results indicate that the higher log likelihood is not artificially inflated by additional flexibility. Rather, the new ingredients of the model do improve the fitting in a meaningful way. Our main model also provides the best overall fit to the forward curve with the smaller measurement errors. All the evidence points to the conclusion that the data favor our main model over these alternative model specifications.

Figure 7 provides some visual evidence by comparing the observed data in blue dots with various model-implied curves. The left panel plots the average forward rates in 2006 when

Figure 7: Forward curves

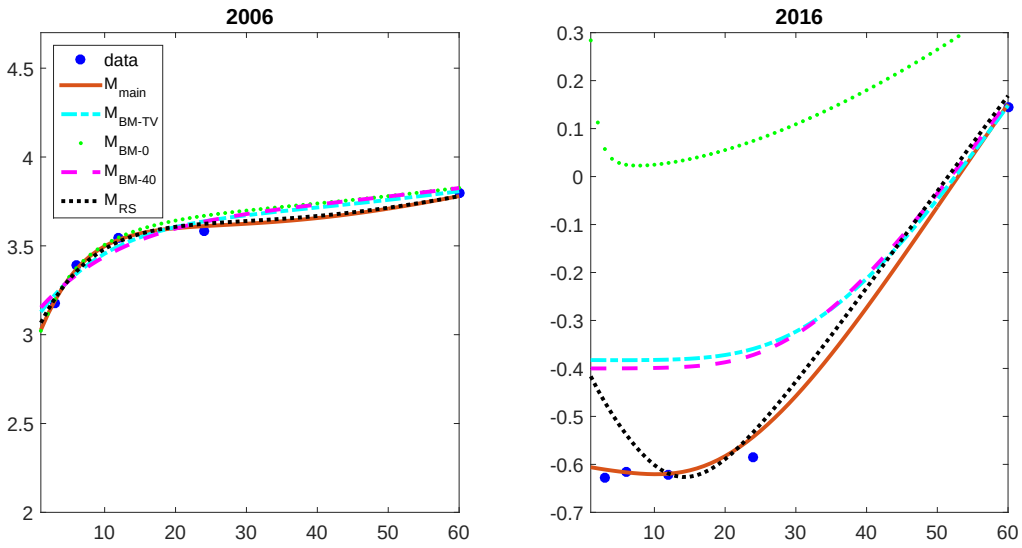

Notes: Left panel: average observed and fitted forward curve in the year 2006; right panel: average observed and fitted forward curve in the year 2016; blue dots: observed data; red solid line: our main model M_{main}; cyan dotted-dashed line: benchmark model M_{BM-TV} with exogenously varying lower bound; green dotted line: benchmark model M_{BM-0} with a constant lower bound at zero; magenta dashed line: benchmark model M_{BM-40} with a constant lower bound at -40 basis points; black dotted line: M_{RS} without spread. X-axis: maturity in month; Y-axis: interest rates in percentage points.

the ELB was not binding, and all the models fit the data similarly well. The right panel shows that in 2016, when the ELB was binding and the spread was over 20 basis points on average, our preferred model M_{main} fits the short end of the term structure significantly better.

Discussion on choice of exogenous lower bound For the benchmark models existing in the literature, although the lower bound is exogenously given, its choice is not innocuous. For example, the only difference between M_{BM-0} and M_{BM-40} is the level of the constant lower bound. However, their performances differ dramatically. Their log likelihood differ by around 400. The measurement errors on the short of the curve end at the ELB for M_{BM-0} is over 37 basis points, whereas they are about 13 for M_{BM-40}. The explanation is intuitive: the model M_{BM-0} sets the lower bound artificially at 0, and it does not allow yields or

forward rates lower than 0. Any observed negative yield is considered a measurement error. So, for example, in Figure 7, the average forward rates for maturities from 3 months to 2 years are around -60 basis points in 2016. The model-implied curve in green, however, is above 0, and obviously is not able to fit the data.

Although all the benchmarks from the literature are not doing nearly as well as our main model, among them, the model with an exogenously moving lower bound M_{BM-TV} does the best, based on likelihood and information criteria. In terms of measurement errors, M_{BM-TV} fits the longer end better, whereas the model with a constant lower bound at -40 basis points M_{BM-40} fits the shorter end better.

Importance of modeling components The comparison between the benchmark model M_{BM-TV} and the intermediate model M_{RS} demonstrates the importance of forward-looking agents. The paths of the lower bound are the same in the two models. The difference lies in how agents form expectations: agents are fully forward-looking in M_{RS}, anticipating future changes in the lower bound, and incorporate this information into their pricing decisions. In M_{BM-TV}, agents do not learn from experience and always think the lower bound will stay at the current level indefinitely even after seeing it move repeatedly.

The model M_{RS} with forward-looking agents has a much higher likelihood, and lower information criteria and measurement errors. The right panel of Figure 7 shows that although it is not able to fit the three-month-ahead forward rate, it does a better job fitting the six-month-ahead and one- to two-year-ahead forward rates, because the forward-looking aspect allows the curve to go down when maturity increases. This is not feasible in the benchmark model M_{BM-TV}. The implied forward curves in cyan stay flat, missing the entire short end.

Both Table 5 and Figure 7 show that compared to M_{RS}, M_{main} is doing better in terms of all the dimensions we investigate. This comparison demonstrates the importance of the time-varying spread, which allows the short end of the forward curve to be decoupled from the policy lower bound. This data feature is evident in Figure 3. For example, in 2016, the

Figure 8: Shadow rate

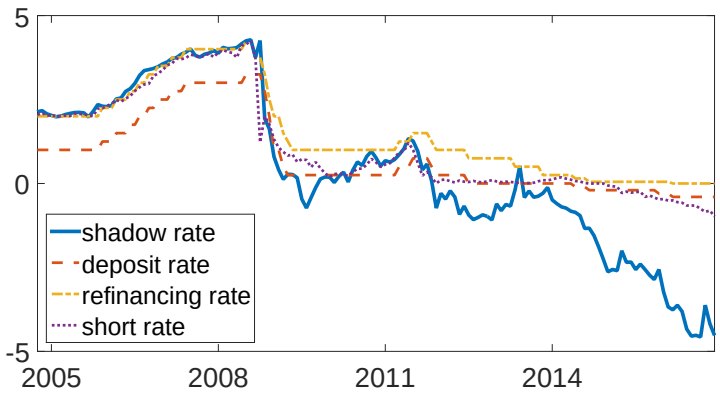

Notes: Blue solid line: shadow rate in our main model; red dashed line in the top panel: deposit rate; yellow dotted-dashed line: refinancing rate; purple dotted line: one-month short-term interest rate. X-axis: time; Y-axis: interest rates in percentage points. Sample spans from September 2004 to December 2016.

policy lower bound was at -0.4%, whereas the average three-month-ahead forward rate was less than -0.6%. Without a spread, M_{RS} has difficulty fitting the three-month maturity.

The overall conclusion is that both modeling components are crucial to model the term structure of the Euro area government bond yield curve.

6.3 Shadow rate

The shadow rate is an object of interest from this model. See Bullard (2012), Altig (2014), Hakkio and Kahn (2014), and Wu and Zhang (2016) for discussions on its potential usefulness for summarizing monetary policy. Figure 8 plots the filtered shadow rate from our main model M_{main} in the solid blue line, together with the deposit rate in the dashed red line, the refinancing rate in the dotted-dashed yellow line, and the short rate in the dotted purple line. When interest rates were higher, the shadow rate tracked the dynamics of the refinancing rate and short rate, which are the policy rate and the short end of the yield curve, respectively. When the deposit rate dropped to 0.25% in 2009 for the first time, the shadow rate dipped negative for a brief period of four months. At the end of 2011, the deposit rate went back down to 0.25% after eight months at higher levels, and the shadow rate has since become

negative. This observation implies that although the ELB was not officially binding, it was practically binding in the low interest rate environment.

Since the deposit rate was lowered to zero in July 2012, the variation in the policy rates or the short rate has been limited, whereas the shadow rate has displayed its own dynamics. When the deposit rate was at 0, the shadow rate fluctuated between 0 and -1%. The shadow rate has trended down since the ECB introduced the negative interest rate policy intending further easing. When the deposit rate dropped from 0 to -40 basis points, the shadow rate decreased from around -1% to almost -5%.

6.4 Term premium

Term premium is one of the focal points for the term structure literature. See, for example, Duffee (2002), Wright (2011), Bauer et al. (2012, 2014), and Creal and Wu (2016). We compute the 10-year term premium for the Euro area from our main model, and plot them in the blue line in Figure 9.

The term premium have trended down since 2009. At the ELB, we observe some negative term premium. This observation can mainly be attributed to the QE programs, which purchase longer-term government bonds and reduce yields through the term premium channel. For empirical evidence, see Gagnon et al. (2011), Krishnamurthy and Vissing-Jorgensen (2011), and Hamilton and Wu (2012a).

A new question in our context is whether the time variation of the policy lower bound incurs an additional term premium on the longer-term yield or forward rate. To address this question, we extend our main model by allowing the physical and risk-neutral dynamics for the regime-switching part to be different. Specifically, the two dynamics follow the same process as described in Subsection 4.1, but with different parameters: (p, π) for the physical dynamics, and $(p^{\mathbb{Q}}, \pi^{\mathbb{Q}})$ for the risk-neutral dynamics.

The yellow dotted line in Figure 9 plots the regime-switching portions of the term premium, which are essentially zero. This result attributes almost all of the term premium

Figure 9: 10-year term premia

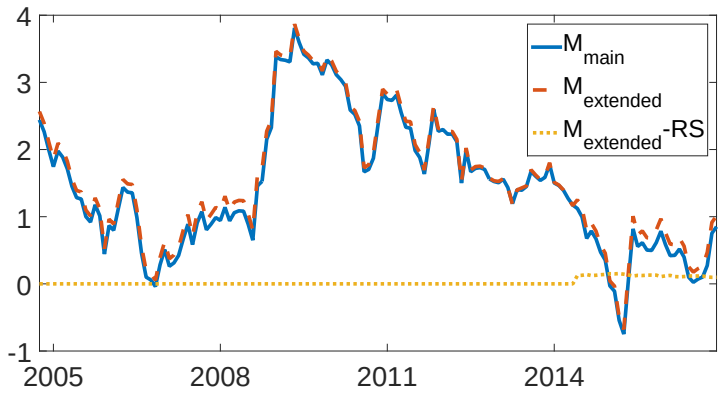

Notes: Yield term premia. Blue solid lines: term premium from our main model; red dashed lines: term premium from the extended model; yellow dotted lines: the regime-switching portions of term premium from the extended model. X-axis: time; Y-axis: interest rates in percentage points. Sample spans from September 2004 to December 2016.

to uncertainty about the underlying latent factors. Moreover, the overall term premium in the extended model in red dashed lines are essentially the same as those in our main model. Hence, the term premium from our main model are robust, and this extension does not make an economic difference.

7 Conclusion

We proposed a new shadow-rate term structure model, which captures the time-varying lower bound that has emerged recently in Europe and Japan. Two main aspects contribute to this time-varying lower bound. First, the deposit rate has moved in a discrete negative grid, and we capture its dynamics with a regime-switching model. In our model, agents are forward looking, anticipate future changes in the deposit rate, and price them into bond prices. Second, a time-varying spread exists between the policy lower bound and the government yield curve, capturing some institutional details. We find both ingredients crucially contribute to the fit of the forward curve and yield curve. Compared to alternative specifications for the lower bound, including the ones proposed in the literature, our new

model fits the data the best.

Our counterfactual policy analyses show that increasing and decreasing the lower bound have asymmetric effects on the yield curve. A 10-basis-point decrease in the ELB lowers the short end of the yield curve by the same amount. The effect decays as the maturity increases, and it amounts to 6.5 to 8.5 basis points at the 10-year horizon. In contrast, a 10-basis-point first raise in the ELB has the strongest effect on the medium maturities between 2 to 4 years, and it increases the 10-year yield by 9 to 14 basis points. These asymmetric responses have important policy implications. The shadow rate fluctuated between 0 and -1% when the deposit rate was at 0. When the deposit rate moved from 0 to -40 basis points, the shadow rate dropped from -1% to -5%. Term premia were higher between 2004 and 2008. It has trended down since 2009, with negative numbers at the ELB, potentially due to QE purchases.

References

Adrian, Tobias, Richard K. Crump, and Emanuel Moench, "Pricing the term structure with linear regressions.," 2012, *110* (1), 110–138.

Altig, Dave, "What is the stance of monetary policy?," *Macroblog, Federal Reserve Bank of Atlanta*, 2 2014.

Ang, Andrew and Geert Bekaert, "Regime Switches in Interest Rates," *Journal of Business & Economic Statistics*, 2002, *20* (2), 163–182.

Bansal, Ravi and Hao Zhou, "Term structure of interest rates with regime shifts," *The Journal of Finance*, 2002, *57* (5), 1997–2043.

Bauer, Michael D. and Glenn D. Rudebusch, "Monetary Policy Expectations at the Zero Lower Bound," *Journal of Money, Credit and Banking*, 2016, *48* (7), 1439–1465.

_ , _ , and Jing Cynthia Wu, "Correcting Estimation Bias in Dynamic Term Structure Models," *Journal of Business & Economic Statistics*, 2012, *30* (3), 454–467.

_ , _ , and _ , "Term Premia and Inflation Uncertainty: Empirical Evidence from an International Panel Dataset: Comment," *American Economic Review*, January 2014, *104* (1), 323–37.

BIS, "Dissonant Markets?," *BIS Quarterly Review September*, 2016.

Black, Fischer, "Interest Rates as Options," *Journal of Finance*, 1995, *50*, 1371–1376.

Borio, Claudio EV, Leonardo Gambacorta, and Boris Hofmann, "The Influence of Monetary Policy on Bank Profitability," 2015. BIS working paper.

Bullard, James, "Shadow interest rates and the stance of U.S. monetary policy," 2012. Annual corporate finance conference.

Christensen, J. H. E. and Glenn D. Rudebusch, "Estimating shadow-rate term structure models with near-zero yields," *Journal of Financial Econometrics*, 2014, *0*, 1–34.

Christensen, Jens H.E., Francis X. Diebold, and Glenn D. Rudebusch, "The affine arbitrage-free class of Nelson-Siegel term structure models.," 2011, *164* (1), 4–20.

Cœuré, Benoît, "Assessing the implications of negative interest rates," in "speech at the Yale Financial Crisis Forum, Yale School of Management, New Haven," Vol. 28 2016.

Creal, Drew D. and Jing Cynthia Wu, "Estimation of affine term structure models with spanned or unspanned stochastic volatility," *Journal of Econometrics*, 2015, *185* (1), 60 – 81.

_ and _ , "Bond risk premia in consumption based models.," 2016. Working paper, University of Chicago, Booth School of Business.

Dai, Qiang, Kenneth J Singleton, and Wei Yang, "Regime shifts in a dynamic term structure model of US treasury bond yields," *Review of Financial Studies*, 2007, *20* (5), 1669–1706.

de Los Rios, Antonio Diez, "A New Linear Estimator for Gaussian Dynamic Term Structure Models," *Journal of Business & Economic Statistics*, 2015, *33* (2), 282–295.

Duffee, Gregory R., "Term premia and interest rate forecasts in affine models," 2002, *57* (1), 405–443.

Gagnon, Joseph, Mattew Raskin, Julie Remache, and Brian Sack, "The Financial Market Effects of the Federal Reserve's Large-Scale Asseet Purchase," *International Journal of Central Banking*, 2011, *7*, 3–43.

Hakkio, Craig S. and George A. Kahn, "Evaluating monetary policy at the zero lower bound," *The Macro Bulletin, Federal Reserve Bank of Kansas City*, 7 2014.

Hamilton, James D., "A New Approach to the Economic Analysis of Nonstationary Time Series and the Business Cycle," *Econometrica*, 1989, *57* (2), 357–384.

_ , *Time Series Analysis*, Princeton, New Jersey: Princeton University Press, 1994.

_ **and Jing Cynthia Wu**, "The effectiveness of alternative monetary policy tools in a zero lower bound environment," 2012, *44 (s1)*, 3–46.

_ **and** _ , "Identification and estimation of Gaussian affine term structure models.," 2012, *168* (2), 315–331.

_ **and** _ , "Testable Implications of Affine Term Structure Models," *Journal of Econometrics*, 2014, *178*, 231–242.

Ichiue, Hibiki and Yoichi Ueno, "Estimating Term Premia at the Zero Bound : an Analysis of Japanese, US, and UK Yields," 2013. Bank of Japan Working Paper.

Jobst, Andreas and Huidan Lin, "Negative Interest Rate Policy (NIRP): Implications for Monetary Transmission and Bank Profitability in the Euro Area," 2016. IMF working paper.

Joslin, Scott, Kenneth J. Singleton, and Haoxiang Zhu, "A new perspective on Gaussian affine term structure models," 2011, *27*, 926–970.

Kim, Don H. and Kenneth J. Singleton, "Term Structure Models and the Zero Bound: an Empirical Investigation of Japanese Yields," *Journal of Econometrics*, 2012, *170*, 32–49.

Kortela, Tomi, "A shadow rate model with time-varying lower bound of interest rates," 2016. Bank of Finland Research Discussion Paper.

Krippner, Leo, "A Tractable Framework for Zero Lower Bound Gaussian Term Structure Models," August 2013. Australian National University CAMA Working Paper 49/2013.

Krishnamurthy, Arvind and Annette Vissing-Jorgensen, "The Effects of Quantitative Easing on Interest Rates: Channels and Implications for Policy," *Brookings Papers on Economic Activity*, 2011, *2*, 215–265.

Lemke, Wolfgang and Andreea L Vladu, "Below the zero lower bound: A shadow-rate term structure model for the euro area," 2016. Deutsche Bundesbank Discussion Paper.

Wright, Jonathan H., "Term premia and inflation uncertainty: empirical evidence from an international panel dataset.," 2011, *101(4)*, 1514–1534.

Wu, Jing Cynthia and Fan Dora Xia, "Measuring the macroeconomic impact of monetary policy at the zero lower bound.," 2016, *48* (2-3), 253–291.

_ **and Ji Zhang**, "A Shadow Rate New Keynesian Model," 2016. NBER Working Paper No. 22856.

Appendix A Joint dynamics of the lower bound

This section derives the matrix form of (4.6) - (4.7). Define

$$\xi_{t+n|t} = \begin{bmatrix} P_t^{\mathbb{Q}}(\Delta_{t+n} = +1; \underline{r}^d_{t+n} = 0) \\ P_t^{\mathbb{Q}}(\Delta_{t+n} = +1; \underline{r}^d_{t+n} = -10) \\ \vdots \\ P_t^{\mathbb{Q}}(\Delta_{t+n} = +1; \underline{r}^d_{t+n} = -\underline{R}) \\ P_t^{\mathbb{Q}}(\Delta_{t+n} = -1; \underline{r}^d_{t+n} = 0) \\ P_t^{\mathbb{Q}}(\Delta_{t+n} = -1; \underline{r}^d_{t+n} = -10) \\ \vdots \\ P_t^{\mathbb{Q}}(\Delta_{t+n} = -1; \underline{r}^d_{t+n} = -\underline{R}) \end{bmatrix}.$$

Its dynamics are given by

$$\xi_{t+n|t} \quad = \quad \Pi \xi_{t+n-1|t},$$

where

$$\Pi = \begin{bmatrix} p^{\mathbb{Q}}\Pi_{+1} & (1-p^{\mathbb{Q}})\Pi_{+1} \\ (1-p^{\mathbb{Q}})\Pi_{-1} & p^{\mathbb{Q}}\Pi_{-1} \end{bmatrix}$$

and

$$\Pi_{+1} \quad = \quad \begin{bmatrix} 1 & 1-\pi^{\mathbb{Q}} & 0 & 0 & \dots & 0 & 0 \\ 0 & \pi^{\mathbb{Q}} & 1-\pi^{\mathbb{Q}} & 0 & \dots & 0 & 0 \\ 0 & 0 & \pi^{\mathbb{Q}} & 1-\pi^{\mathbb{Q}} & \dots & 0 & 0 \\ 0 & 0 & 0 & \pi^{\mathbb{Q}} & \dots & 0 & 0 \\ \vdots & \vdots & \vdots & \vdots & & \vdots & \vdots \\ 0 & 0 & 0 & 0 & \dots & \pi^{\mathbb{Q}} & 1-\pi^{\mathbb{Q}} \\ 0 & 0 & 0 & 0 & \dots & 0 & \pi^{\mathbb{Q}} \end{bmatrix}$$

$$\Pi_{-1} \quad = \quad \begin{bmatrix} 1 & 0 & 0 & 0 & \dots & 0 & 0 \\ 0 & \pi^{\mathbb{Q}} & 0 & 0 & \dots & 0 & 0 \\ 0 & 1-\pi^{\mathbb{Q}} & \pi^{\mathbb{Q}} & 0 & \dots & 0 & 0 \\ 0 & 0 & 1-\pi^{\mathbb{Q}} & \pi^{\mathbb{Q}} & \dots & 0 & 0 \\ \vdots & \vdots & \vdots & \vdots & & \vdots & \vdots \\ 0 & 0 & 0 & 0 & \dots & \pi^{\mathbb{Q}} & 0 \\ 0 & 0 & 0 & 0 & \dots & 0 & 1 \end{bmatrix}.$$

Appendix B Deriving pricing formula

Appendix B.1 General form

As shown in Wu and Xia (2016), the forward rate is

$$\begin{aligned} f_{nt} &\approx \mathbb{E}_t^{\mathbb{Q}}[r_{t+n}] - \frac{1}{2}\left(\mathbb{V}\text{ar}_t^{\mathbb{Q}}\left[\sum_{j=1}^{n} r_{t+j}\right] - \mathbb{V}\text{ar}_t^{\mathbb{Q}}\left[\sum_{j=1}^{n-1} r_{t+j}\right]\right) \\ &\approx \mathbb{E}_t^{\mathbb{Q}}[\max(s_{t+n}, \underline{r}_{t+n})] - P_t^{\mathbb{Q}}(s_{t+n} \geq \underline{r}_{t+n}) \times \frac{1}{2}\left(\mathbb{V}\text{ar}_t^{\mathbb{Q}}\left[\sum_{j=1}^{n} s_{t+j}\right] - \mathbb{V}\text{ar}_t^{\mathbb{Q}}\left[\sum_{j=1}^{n-1} s_{t+j}\right]\right). \end{aligned} \tag{B.1}$$

The right-hand side equals

$$\int \left[-P_t^{\mathbb{Q}}(s_{t+n} \geq \underline{r}_{t+n} | \underline{r}_{t+n}) \times \frac{1}{2}\left(\mathbb{V}\text{ar}_t^{\mathbb{Q}}\left[\sum_{j=1}^{n} s_{t+j}\right] - \mathbb{V}\text{ar}_t^{\mathbb{Q}}\left[\sum_{j=1}^{n-1} s_{t+j}\right]\right) \right.$$
$$\left. + \mathbb{E}_t^{\mathbb{Q}}[\max(s_{t+n}, \underline{r}_{t+n} | \underline{r}_{t+n})] \right] P_t^{\mathbb{Q}}(\underline{r}_{t+n}) d\underline{r}_{t+n}.$$

According to Wu and Xia (2016), the expression inside the integral conditioning on the lower bound equals

$$\underline{r}_{t+n} + \tilde{\sigma}_n^{\mathbb{Q}} g\left(\frac{a_n + b_n' X_t - \underline{r}_{t+n}}{\tilde{\sigma}_n^{\mathbb{Q}}}\right).$$

Hence, we obtain (3.5).

Appendix B.2 Main model

First,

$$P_t^{\mathbb{Q}}(s_{t+n} - sp_{t+n}) \sim N\big(\bar{a}_n + b_n' X_t - c_n sp_t, (\sigma_n^{\mathbb{Q}})^2\big),$$

where $\bar{a}_n \equiv \delta_0 + \delta_1' \left(\sum_{j=0}^{n-1} \left(\rho^{\mathbb{Q}}\right)^j\right) \mu^{\mathbb{Q}}$. The first term on the right-hand side of (B.1) is

$$\begin{aligned} \mathbb{E}_t^{\mathbb{Q}}[r_{t+n}] &= \mathbb{E}_t^{\mathbb{Q}}[\max(\underline{r}_{t+n}^d + sp_{t+n}, s_{t+n})] \\ &= \mathbb{E}_t^{\mathbb{Q}}[\max(\underline{r}_{t+n}^d, s_{t+n} - sp_{t+n}) + sp_{t+n}] \\ &= \sum_{\underline{r}_{t+n}^d} P_t^{\mathbb{Q}}(\underline{r}_{t+n}^d) \mathbb{E}_t^{\mathbb{Q}}[\max(\underline{r}_{t+n}^d, s_{t+n} - sp_{t+n}) | \underline{r}_{t+n}^d] + \mathbb{E}_t^{\mathbb{Q}}(sp_{t+n}) \\ &= \sum_{\underline{r}_{t+n}^d} P_t^{\mathbb{Q}}(\underline{r}_{t+n}^d) \left(\underline{r}_{t+n}^d + \sigma_n^{\mathbb{Q}} g\left(\frac{\bar{a}_n + b_n' X_t - c_n sp_t - \underline{r}_{t+n}^d}{\sigma_n^{\mathbb{Q}}}\right)\right) + sp_t, \end{aligned}$$

where the derivation for the last equal sign follows Wu and Xia (2016).

The second term of (B.1) is

$$\begin{aligned}
&\frac{1}{2}\left(\mathbb{V}\mathrm{ar}_t^{\mathbb{Q}}\left[\sum_{j=1}^{n} r_{t+j}\right] - \mathbb{V}\mathrm{ar}_t^{\mathbb{Q}}\left[\sum_{j=1}^{n-1} r_{t+j}\right]\right) \\
\approx\ & P_t^{\mathbb{Q}}(s_{t+n} - sp_{t+n} \geq \underline{r}_{t+n}^d) \times \frac{1}{2}\left(\mathbb{V}\mathrm{ar}_t^{\mathbb{Q}}\left[\sum_{j=1}^{n} s_{t+j}\right] - \mathbb{V}\mathrm{ar}_t^{\mathbb{Q}}\left[\sum_{j=1}^{n-1} s_{t+j}\right]\right) \\
=\ & \sum_{\underline{r}_{t+n}^d} P_t^{\mathbb{Q}}(\underline{r}_{t+n}^d) P_t^{\mathbb{Q}}(s_{t+n} - sp_{t+n} \geq \underline{r}_{t+n}^d | \underline{r}_{t+n}^d) \times \frac{1}{2}\left(\mathbb{V}\mathrm{ar}_t^{\mathbb{Q}}\left[\sum_{j=1}^{n} s_{t+j}\right] - \mathbb{V}\mathrm{ar}_t^{\mathbb{Q}}\left[\sum_{j=1}^{n-1} s_{t+j}\right]\right) \\
=\ & \sum_{\underline{r}_{t+n}^d} P_t^{\mathbb{Q}}(\underline{r}_{t+n}^d) \Phi\left(\frac{\bar{a}_n + b_n' X_t - c_n sp_t - \underline{r}_{t+n}^d}{\sigma_n^{\mathbb{Q}}}\right) \times (\bar{a}_n - a_n),
\end{aligned}$$

where the first approximation sign and last equal sign follow Wu and Xia (2016).

Adding them together yields (4.10):

$$\begin{aligned}
f_{nt} \approx\ & \sum_{\underline{r}_{t+n}^d} P_t^{\mathbb{Q}}(\underline{r}_{t+n}^d) \left(\underline{r}_{t+n}^d + \sigma_n^{\mathbb{Q}} g\left(\frac{a_n + b_n' X_t - c_n sp_t - \underline{r}_{t+n}^d}{\sigma_n^{\mathbb{Q}}}\right)\right) + c_n sp_t \\
=\ & \sum_{\underline{r}_{t+n}^d} P_t^{\mathbb{Q}}(\underline{r}_{t+n}^d) \left(c_n sp_t + \underline{r}_{t+n}^d + \sigma_n^{\mathbb{Q}} g\left(\frac{a_n + b_n' X_t - c_n sp_t - \underline{r}_{t+n}^d}{\sigma_n^{\mathbb{Q}}}\right)\right),
\end{aligned}$$

where the approximation follows Wu and Xia (2016).

Appendix C Estimation

Appendix C.1 Likelihood for observed state variables

The observed state variables are $(\underline{r}_t^d, \Delta_t)$. The likelihood for $\underline{r}_t^d$ and Δ_t is

$$\begin{aligned}
& P(\underline{r}_{2:T}^d, \Delta_{2:T} | \underline{r}_1^d, \Delta_1) \\
=\ & \Pi_{t=2}^T P(\underline{r}_t^d, \Delta_t | \underline{r}_{1:t-1}^d, \Delta_{1:t-1}) \\
=\ & \Pi_{t=2}^T P(\underline{r}_t^d, \Delta_t | \underline{r}_{t-1}^d, \Delta_{t-1}) \\
=\ & \Pi_{t=2}^T P(\underline{r}_t^d | \Delta_t, \underline{r}_{t-1}^d) P(\Delta_t | \Delta_{t-1}) \\
=\ & p^{N_1}(1-p)^{T-1-N_1} \pi^{N_2} (1-\pi)^{(\tilde{T}-N_2)},
\end{aligned}$$

where N_1 is the number of periods that Δ_t does not change, N_2 is the number of periods that $\underline{r}_t^d$ does not change, T is the total number of periods, and $\tilde{T}$ is the number of periods $\underline{r}_t^d \neq 0$. The log likelihood value for $(\underline{r}_t^d, \Delta_t)$ is

$$\begin{aligned}
\mathcal{L}_1 &= \log(P(\underline{r}_{2:T}^d, \Delta_{2:T} | \underline{r}_1^d, \Delta_1)) \\
&= N_1 log(p) + (T - 1 - N_1) log(1-p) + N_2 log(\pi) + (\tilde{T} - N_2) log(1-\pi).
\end{aligned}$$

Taking first-order derivatives of the log likelihood with respect to p and π and setting them to 0 yields

$$\hat{p} = \frac{N_1}{T-1}$$
$$\hat{\pi} = \frac{N_2}{\tilde{T}}.$$

Appendix C.2 Extended Kalman filter

Define $\mathcal{X}_t \equiv [X_t', sp_t]'$. The transition equations for latent factors $\mathcal{X}_t$ are in (3.2) and (4.9). Stack the observation equation (5.1) for all seven maturities:

$$F_t^o = F\left(\mathcal{X}_t, \underline{r}_t^d, \Delta_t\right) + \eta_t \quad \eta_t \sim N(0, \omega^2 I_7).$$

Approximate the conditional distribution of $\mathcal{X}_t$ with $\mathcal{X}_t | F_{1:t}^o, \underline{r}_{1:t}^d, \Delta_{1:t}, \sim N(\hat{\mathcal{X}}_{t|t}, P_{t|t})$. Initializing with $\hat{\mathcal{X}}_{0|0} = (I_4 - \tilde{\rho})^{-1}\tilde{\mu}$ and $vec(P_{0|0}) = (I_{16} - (\tilde{\rho} \otimes \tilde{\rho}))^{-1} vec(\tilde{\Sigma}\tilde{\Sigma}')$, we update $\hat{\mathcal{X}}_{t|t}$ and $P_{t|t}$ recursively according to

$$\begin{aligned}
\hat{\mathcal{X}}_{t|t-1} &= \tilde{\mu} + \tilde{\rho}\hat{\mathcal{X}}_{t-1|t-1}, \\
P_{t|t-1} &= \tilde{\rho} P_{t-1|t-1}\tilde{\rho}' + \tilde{\Sigma}\tilde{\Sigma}', \\
\hat{F}_{t|t-1}^o &= F(\hat{\mathcal{X}}_{t|t-1}, \underline{r}_t^d, \Delta_t), \\
H_t &= \left(\frac{\partial F(\mathcal{X}_t, \underline{r}_t^d, \Delta_t)}{\partial \mathcal{X}_t'}\bigg|_{\mathcal{X}_t = \hat{\mathcal{X}}_{t|t-1}} \right)', \\
K_t &= P_{t|t-1} H_t \left(H_t' P_{t|t-1} H_t + \omega I_7 \right)^{-1}, \\
\hat{\mathcal{X}}_{t|t} &= \hat{\mathcal{X}}_{t|t-1} + K_t(F_t^o - \hat{F}_{t|t-1}^o), \\
P_{t|t} &= \left(I_4 - K_t H_t' \right) P_{t|t-1},
\end{aligned}$$

where H_t' stacks $\sum_{\underline{r}_{t+n}^d} \left(P_t^{\mathbb{Q}}(\underline{r}_{t+n}^d) \Phi \left(\frac{a_n + [b_n', c_n]\hat{\mathcal{X}}_{t|t-1} - \underline{r}_{t+n}^d}{\sigma_n^{\mathbb{Q}}} \right) \times [b_n', c_n] \right)$ for all maturities, and

$$\tilde{\mu} = \begin{bmatrix} \mu \\ 0 \end{bmatrix}, \tilde{\rho} = \begin{bmatrix} \rho & 0_{3\times 1} \\ 0_{1\times 3} & \rho_{sp} \end{bmatrix}, \tilde{\Sigma} = \begin{bmatrix} \Sigma & 0_{3\times 1} \\ 0_{1\times 3} & \sigma_{sp} \end{bmatrix}.$$

The conditional log likelihood is

$$\begin{aligned}
\mathcal{L}_2 &= \log(P(F_{2:T}^o | F_1^o, \underline{r}_{2:T}^d, \Delta_{2:T})) \\
&= -\frac{7(T-1)}{2}\log 2\pi - \frac{1}{2}\sum_{t=2}^{T} \log |H_t' P_{t|t-1} H_t + \omega^2 I_7| \\
&\quad -\frac{1}{2}\sum_{t=2}^{T} (F_t^o - F(\hat{\mathcal{X}}_{t|t-1}, \underline{r}_t^d, \Delta_t)' \left(H_t' P_{t|t-1} H_t + \omega^2 I_7 \right)^{-1} (F_t^o - F(\hat{\mathcal{X}}_{t|t-1}, \underline{r}_t^d, \Delta_t).
\end{aligned}$$

Table C.1: Observation equations for alternative models

model	observation equation
M_{BM-TV}	$\underline{r}_t^d + \tilde{\sigma}_n^{\mathbb{Q}} g\left(\frac{a_n + b_n' X_t - \underline{r}_t^d}{\tilde{\sigma}_n^{\mathbb{Q}}}\right)$
M_{BM-0}	$\underline{r} + \tilde{\sigma}_n^{\mathbb{Q}} g\left(\frac{a_n + b_n' X_t - \underline{r}}{\tilde{\sigma}_n^{\mathbb{Q}}}\right), \underline{r} = 0$
M_{BM-40}	$\underline{r} + \tilde{\sigma}_n^{\mathbb{Q}} g\left(\frac{a_n + b_n' X_t - \underline{r}}{\tilde{\sigma}_n^{\mathbb{Q}}}\right), \underline{r} = -40$ basis points
M_{RS}	$\sum_{\underline{r}_{t+n}^d} P_t^{\mathbb{Q}}(\underline{r}_{t+n}^d)\left(\underline{r}_{t+n}^d + \tilde{\sigma}_n^{\mathbb{Q}} g\left(\frac{a_n + b_n' X_t - \underline{r}_{t+n}^d}{\tilde{\sigma}_n^{\mathbb{Q}}}\right)\right)$
model	derivative
M_{BM-TV}	$\Phi\left(\frac{a_n + b_n' \hat{X}_{t\|t-1} - \underline{r}_t^d}{\tilde{\sigma}_n^{\mathbb{Q}}}\right) \times b_n'$
M_{BM-0}	$\Phi\left(\frac{a_n + b_n' \hat{X}_{t\|t-1} - \underline{r}}{\tilde{\sigma}_n^{\mathbb{Q}}}\right) \times b_n', \underline{r} = 0$
M_{BM-40}	$\Phi\left(\frac{a_n + b_n' \hat{X}_{t\|t-1} - \underline{r}}{\tilde{\sigma}_n^{\mathbb{Q}}}\right) \times b_n', \underline{r} = -40$basis points
M_{RS}	$\sum_{\underline{r}_{t+n}^d} P_t^{\mathbb{Q}}(\underline{r}_{t+n}^d)\Phi\left(\frac{a_n + b_n' \hat{X}_{t\|t-1} - \underline{r}_{t+n}^d}{\tilde{\sigma}_n^{\mathbb{Q}}}\right) \times b_n'$

Notes: Top panel: observation equations for alternative model specifications, which are components of $F\left(X_t, \underline{r}_t^d, \Delta_t\right)$; bottom panel: derivatives, components of H_t.

The likelihood of the model is the sum of the two components:

$$\begin{aligned} \mathcal{L} &= \log(P(F_{2:T}^o, \underline{r}_{2:T}^d, \Delta_{2:T} | F_1^o, \underline{r}_1^d, \Delta_1)) \\ &= \mathcal{L}_1 + \mathcal{L}_2. \end{aligned}$$

Appendix C.3 Alternative models

None of the alternative models allows a spread: $sp_t = 0$. Hence, $\mathcal{X}_t = X_t$, and $\tilde{\mu} = \mu$, $\tilde{\rho} = \rho$, and $\tilde{\Sigma} = \Sigma$. Observation equations and their derivatives are described in Table C.1. $\mathcal{L}_1$ only applies to M_{RS}, and is 0 for all the benchmark models.